Impact of non-eccentric gravitational waveforms on eccentric gravitational wave searches with LISA

A Dissertation Submitted
in Partial Fulfilment of the Requirements
for the

MASTER OF SCIENCE

in

PHYSICS

by

Akshita Mittal
(Roll No. IMS19027)

to

SCHOOL OF PHYSICS
INDIAN INSTITUTE OF SCIENCE EDUCATION AND RESEARCH
THIRUVANANTHAPURAM - 695 551, INDIA

November 23, 2023

I Abstract

The eccentricity of binary black hole (BBH) mergers is predicted to be an indicator of the history of their formation. Eccentricity, in particular, is a strong signature of dynamical formation rather than formation by stellar evolution in isolated stellar systems. In this thesis, we investigate the significance of using current quasi-circular waveform templates in Bayesian parameter estimation (PE) for eccentric signals. Unlike previous studies, we consider the evolution of both spin and eccentricity in our analysis. In this phase, we create a signal from a massive binary black hole binary (MBHB) and then project it onto the arms of the Laser Interferometer Space Antenna (LISA). This involves employing time-delay interferometry (TDI) expressions to mitigate laser frequency noise. We obtain time and frequency domain signals for PE, which are presented in Section V.

Keywords: *Gravitational waves, LISA, milli-hertz, eccentricity, time-delay interferometry*

II Introduction

As of 2023, the Laser Interferometer Gravitational-wave Observatory (LIGO) and the Virgo observatory have detected gravitational wave (GW) signals from hundreds of BBH mergers. With the next generation of ground-based detectors like the Einstein Telescope (ET) and the Cosmic Explorer (CE), along with space-based LISA and TianQin coming up, we will see an increase in detection rates, particularly at lower frequencies. With these upcoming detectors and the influx of a wide range of data, we will require updated waveform models and data analysis methods to study the sources.

1. About LISA

LISA is the 3rd large mission of the ESA program Cosmic Vision with the goal of detecting GWs in the mHz regime. LISA detects GWs by measuring the relative distance between two freely falling test masses in different spacecraft using laser interferometry. The detector system is expected to have three different spacecraft separated by 2.5 million km placed in a triangular formation—the orbits are chosen so that this triangle is as equilateral as possible. However, celestial dynamics cause the arm lengths to differ from each other and cause a relative drift in the satellites of up to 10m/s. These unequal and time-varying lengths cause the detector to be strongly affected by laser frequency noise.

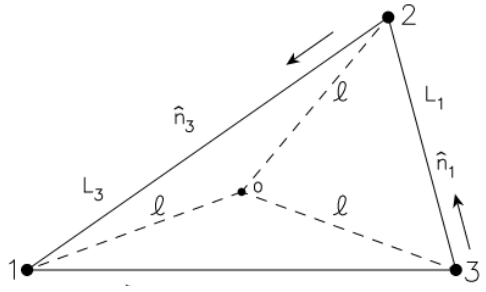

Figure 1: Schematic LISA configuration taken from [1]. Each spacecraft numbered 1-3 is equidistant from point O in the plane of the spacecraft. The distances between spacecraft are L_1, L_2 and L_3, with L_i being opposite spacecraft i.

2. Why eccentricity?

Current extraction of GW signals all use circular orbital waveform templates, because the evolution of binary systems is generally considered to circularize due to GW radiation, i.e., they have negligible eccentricity when entering the LIGO detection band. However, a GW observation with a negligible eccentricity in the hecto-hertz band may have significant eccentricity in the space-based observation window. Space-based detectors are sensitive in a lower frequency band and could observe BBHs for years (4 years for LISA), instead of seconds for ground-based detectors. This makes space-based observatories capable of unveiling the evolution of eccentricity and spin of BBH systems. Additionally, LISA will particularly focus on massive binary systems that have thus far escaped detection.

Eccentricity is a smoking gun for the formation channels of binaries. Understanding the evolution of eccentricity of a binary in a globular cluster can hence clearly describe its dynamical interactions with other bodies in the cluster [3]. Different formation channels have different eccentricity distributions, and the systems that undergo two-body-mergers (mergers *between* two hardening interactions), as shown in Fig. 2, will be relevant for LISA [2].

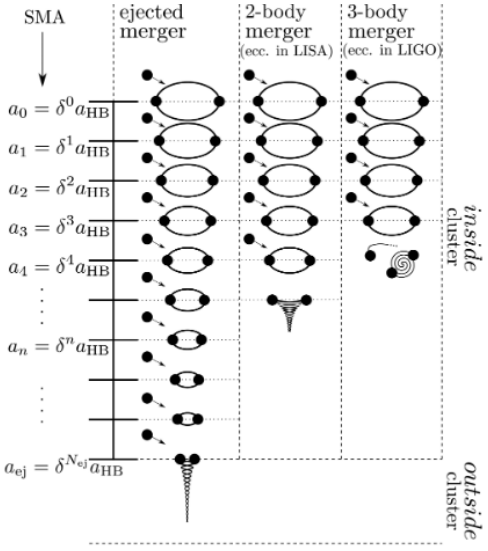

Figure 2: Three different dynamical pathways for the formation of merging BBHs–each results in a different BBH merger. Image taken from [2].

3. Aim

The goal of this project is to study the consequences of the neglect of eccentricity for LISA, in terms of systematic biases caused in the PE of the source. We will focus on MBHB systems with masses of the order of $\mathcal{O}(10^6)M_\odot$. As target waveforms, we consider signals with non-zero spins and eccentricities $e \leq 0.3$ [4], and employ TDI for LISA that cancels out the laser phase noise from different arms and constructs particular combinations to make virtual equal-arm interferometers [5].

In the next phase of the project, we plan to use a non-eccentric waveform like `IMRPhenomHM` [6] as the template waveform, which produces GW signals for spinning, non-precessing binaries with higher order modes to conduct PE. The presence of eccentricity in the signal is expected to induce a potential shift in the posterior peaks in the distributions obtained after PE. We want to investigate the value of eccentricity at which this shift in the peak becomes statistically significant, i.e., it falls out of the confidence level estimated by the circular waveform.

4. Previous work and motivation

The case of non-spinning eccentric targets has been widely studied. Islam et. al. [7], consider a numerical relativity surrogate model `NRSur2dq1Ecc` of a comparable mass, non-spinning case with eccentricities up to 0.2. More recently, Wang et. al. [8] introduce an archival search in the parameter space of LISA/TianQuin with non-spinning, inspiral-only frequency-domain waveform approximant `EccentricFD`, that includes initial eccentricity up to 0.4. Poisson et al. [9] quantified the accuracy to which circular-orbit templates could capture signals from eccentric binaries in the LIGO band, finding that the signal-to-noise ratio (SNR) loss is significant for eccentricities above 0.1. Mildly eccentric systems can be detected by some pipelines, however, with loss of SNR. Moderately eccentric systems would likely be missed by such pipelines. Ignoring eccentricity could thus lead us to infer other intrinsic parameters of the source with biases.

Our method builds on the prior research conducted on non-spinning, eccentric waveforms, and incorporates spin into the analysis. We simulate a set of eccentric IMR signals using the eccentric branch of the `TEOBResumS` waveform template [10] and generate a signal for an MBHB system detectable by LISA using TDI corrections from `lisa-on-gpu` [11]. In section III, we study the evolution of orbital eccentricity in a Keplerian eccentric orbit. We go on to describe our methods in section IV, including a description of the waveform models we use. In section V, we present our results.

III Evolution of an eccentric orbit

A binary system in an ordinary Keplerian orbit radiates both energy and angular momentum. These are drained from the system resulting in secular changes in its semimajor axis and its ellipticity. In this section, we understand how the semimajor axis and ellipticity of a binary system evolve with time. The conservation of L implies that the orbit lies in a plane; we then introduce polar coordinates (r, ψ) in the plane of the orbit, with the origin on the position of the center of mass. The equation of the orbit is

$$\frac{1}{r} = \frac{1}{R}(1 + e\,cos\,\psi) \tag{1}$$

Here, R is the length scale, e the eccentricity of the orbit, and ψ denotes the angular position along the orbit. $R = pM$, where p is the semi-latus rectum and $M = m_1 + m_2$ is the total mass. ψ is obtained by integrating

$$L = \mu r^2 \dot{\psi} \tag{2}$$

$$\frac{d\psi}{dt} = M^{1/2}\frac{(1 + e\,cos\,\psi)^2}{R} \tag{3}$$

and r is obtained by integrating

$$E = \frac{1}{2}\mu(\dot{r}^2 + r^2\dot{\psi}^2) - \frac{G\mu m}{r} \tag{4}$$

where L is the modulus of the total orbital momentum of the system, E is the energy, and $\mu = \dfrac{m_1 m_2}{m_1 + m_2}$ is the reduced mass.

Making use of 2, 4 and the orbital equation of motion 1, the parametric form of the explicit time dependence of $\psi(t)$ and $r(t)$ is given by

$$cos\,\psi = \frac{cos\,u - e}{1 - e\,cos\,u} \tag{5}$$

$$r = a[1 - e\,cos\,u] \tag{6}$$

where u is called the eccentric anomaly and is related to t by the Kepler equation

$$\beta \equiv u - e\,sin\,u = \omega_0 t \tag{7}$$

The semiaxes of the ellipse are given by

$$a = \frac{R}{1 - e^2}, \quad b = \frac{R}{(1 - e^2)^{1/2}} \tag{8}$$

The orbital elements a and e both decrease as a function of time because the gravitational radiation removes energy and angular momentum of the system. The relevant expressions are adapted from [12].

$$\frac{da}{dt} = -\frac{64}{5}\frac{G^3\mu m^2}{c^5 a^3}\frac{1}{(1 - e^2)^{7/2}}\left(1 + \frac{73}{24}e^2 + \frac{37}{96}e^4\right) \tag{9}$$

$$\frac{de}{dt} = -\frac{304}{15}\frac{G^3\mu m^2}{c^5 a^4}\frac{1}{(1 - e^2)^{5/2}}\left(1 + \frac{121}{304}e^2\right) \tag{10}$$

Equations 3, 9 and 10 determine the orbital motion completely once initial values for a, e and ψ are provided.

IV Methods

1. Eccentric waveforms for LIGO

Fig. 3 shows the effect of eccentricity on the amplitude and phase of a system with the same parameters as GW150914. Here, we have compared the waveform GW150914 for zero eccentricity and $e = 0.2$.

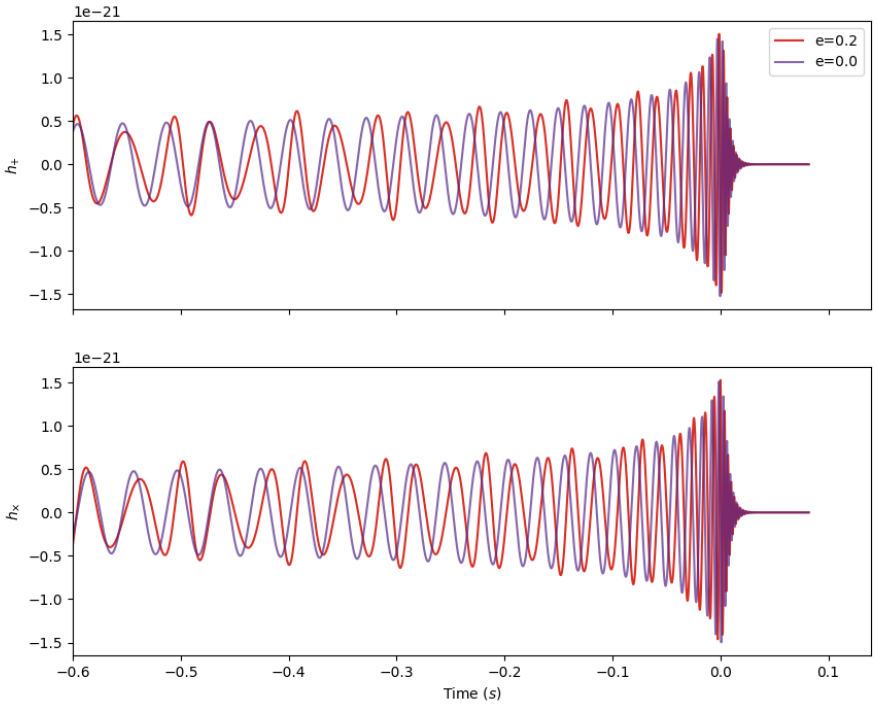

Figure 3: h_+ and $h_\times$ strain for parameters of GW150914. The signals have been cropped to start at $t = -0.6$s, and shifted to merge at the same time to accentuate the difference in amplitude and phase modulation.

2. Parameter details

For the generation of this particular signal, parameters from Ref. [13] are used, and eccentricity, e is varied from 0 to 0.3. The initial frequency is chosen to be 9.112×10^{-4} Hz, and the data is interpolated at $dt = 0.274358$.

Parameter	Value
Total mass, M $(M_\odot)$	3×10^6
Mass ratio, q	2
Spin of primary along orbital angular momentum, χ_1	0.75
Spin of secondary along orbital angular momentum, χ_2	0.62
Luminosity distance, D_L (Mpc)	5.6005×10^4
Inclination, ι	1.22
Ecliptic longitude, λ	3.51
Ecplitic latitude, β	0.29

Table 1: Source parameters for signal generation for an MBHB system.

3. Generation of time-domain signal

The signal is computed using the eccentric branch of the `TEOBResumS` module. To minimize computational costs, we employ geometric units in our calculations and normalize the variables. These normalizations for amplitude, A and time, t are given by

$$A = A \times \frac{q}{(1+q)^2} \times \frac{M \times M_{\odot m}}{D_L \times Mpc_m} \tag{11}$$

$$t = t \times M \tag{12}$$

where $M_{\odot m}$ is the solar mass in meters, and Mpc_m is megaparsecs in meters. The parameters M and D_L appear in equation 11 because the GW signal scales as $\frac{M}{D_L}$.

From `TEOBResumS`, we obtain a time-domain waveform with the plus and cross polarisations. While evaluating the waveform in the frequency domain would be theoretically more efficient, the module faces limitations in handling infinitesimal values of initial frequency and interpolation within the frequency domain.

4. Projection on LISA arms

This is followed by using `ResponseWrapper` from the LISA response tool `lisa-on-gpu` to project the plus and cross polarizations onto LISA. Second-generation TDI corrections provided by the tool are used for this, and the observation period, T, is set to 1 year for $e \leq 2$, and 2 years for $e = 0.25$ and $e = 0.3$. We choose to remove the initial signal from the data that has bad information. Strain is obtained in the AET basis [14]. A, E, and T are quasi-orthogonal TDI channels, where A and E are more sensitive to GWs, while T is a null channel. This is then Fourier transformed to the frequency domain, where the oscillations in amplitude with increasing eccentricity are clearly seen, as shown in Fig. 6.

V Results

In this section, we present the time-domain and frequency-domain signals for eccentricities 0 through 0.3 in Figs 5 and 6.

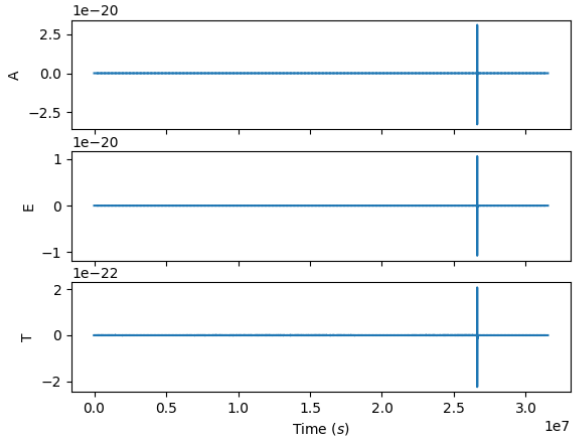

(a) Time-domain signal in A, E and T channels for the MBHB system with $e = 0.2$.

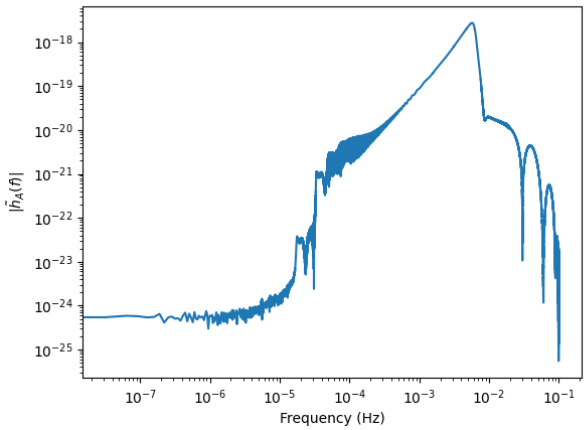

(b) Frequency-domain signal for the MBHB system with $e = 0.2$. Signal below 10^{-4} Hz contains spectral leakage.

Figure 4: Time and frequency domain waveforms for $e = 0.2$ after projection onto LISA arms.

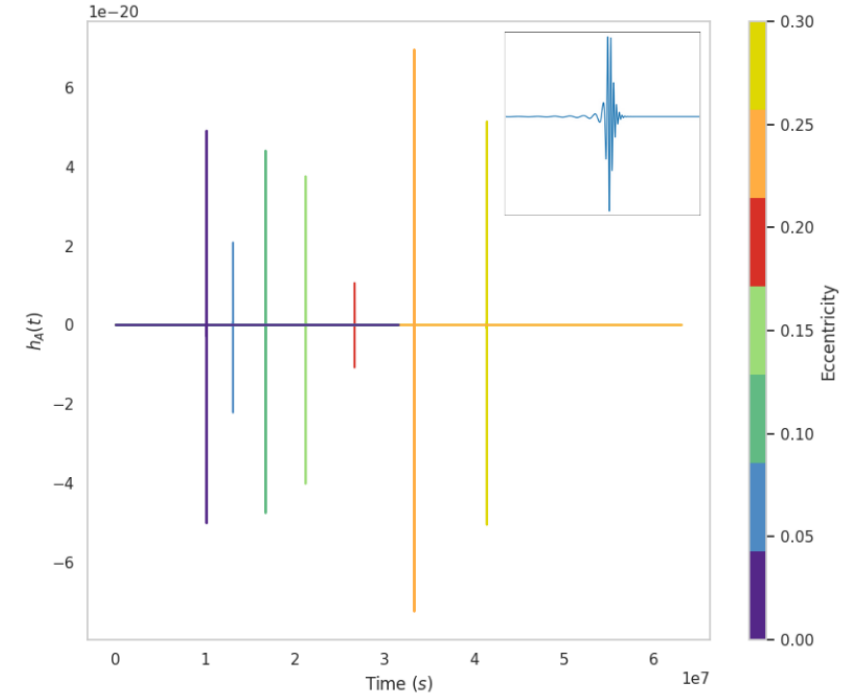

Figure 5: Time-domain signals from eccentricities 0 to 0.3 for an MBHB system after projection onto LISA arms. Only A has been plotted. The seemingly straight lines actually exhibit oscillatory behavior (as depicted in the inlay plot). As expected, the time to merger, t_{coal} increases with an increase in eccentricity because of orbit circularization. The perfectly circular orbit ($e = 0$) has the lowest t_{coal}. The amplitude corresponding to each eccentricity oscillates arbitrarily given the different times of merger because the source localization changes with time due to the time-changing nature of the spacecraft. These fluctuations, however, do not arise if LISA projections are not taken into account.

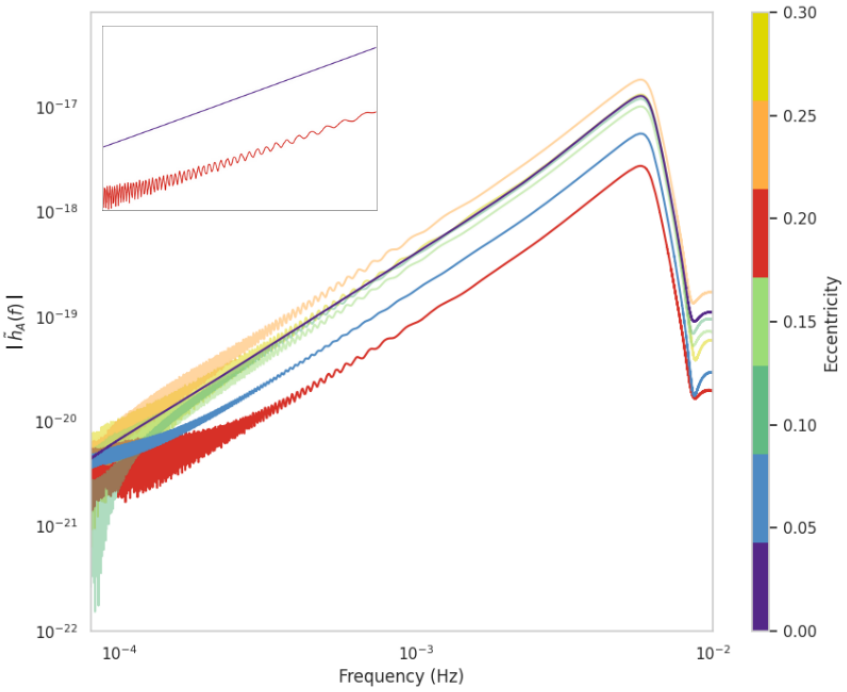

Figure 6: Frequency-domain signals from eccentricities 0 to 0.3 for an MBHB system after projection onto LISA arms plotted in log scale. The amplitude modulation for $e > 0$, as compared to a straight line (purple) for $e = 0$ is an artifact of eccentricity. This distinctive behavior is accentuated in the inlay plot, focusing on eccentricities 0 and 0.2. The difference in amplitude, similar to that seen in Fig. 5 for different eccentricities, arises because of the rotation of the detector plane. This effect becomes apparent due to the distinct values of t_{coal} associated with different eccentricities.

VI Summary

1. Conclusion

In this report, we have studied and generated an MBHB eccentric signal detectable by LISA. We have extended previous studies, which focused on non-spinning searches and non-spinning target signals, to the case of spin searches and targets for the upcoming LISA. We have utilized the 2nd generation TDI variables to cancel out the relative motion of the three LISA spacecraft and minimize the effect of laser frequency noise.

- We see an oscillatory behavior in the amplitude in both time and frequency domains, which is an artifact of eccentricity. This is a consequence of orbit circularization [12].
- The time to merger (t_{coal}) increases with an increase in eccentricity because systems with higher eccentricity take more time to circularize for merger.
- The amplitude fluctuates with different values of eccentricity (Figs 5 and 6), which is expected because of the time-varying movement of the detector plane with respect to the source.

2. Limitations

- As of now, the generation of the `TEOBResumS` signal in the frequency domain remains unrealized.
- The Fourier transform constitutes a significant time-consuming step in our script, and optimizing this process will be crucial for PE purposes.

3. Future Directions

- We will try to optimize the Fourier transform of our time-domain signal, to reduce the time of computation, which will be significant for PE.
- We will incorporate our signal to the LISA pipeline `LISABeta` to conduct PE of this signal with a quasi-circular template.
- This will be followed with a study of the statistical significance of using a quasi-circular template to conduct PE.

VII Acknowledgements

I thank Dr. Soumen Basak and Kallol Dey for fruitful discussions regarding the theory and implementation of the idea. I would like to extend a special thanks to Kallol for making time outside the schedule of this project and driving the project to this stage. I also extend my gratitude to the School of Physics and the Center for High-Performance Computing, IISER-TVM for provision of resources to carry out the project. Additionally, I thank Dr. Rossella Gamba for resolving our doubts and queries about the `TEOBResumS` module.

References

[1] Thomas A. Prince et al. "LISA optimal sensitivity". In: *Physical Review D* 66.12 (Dec. 17, 2002), p. 122002. ISSN: 0556-2821, 1089-4918. DOI: 10.1103/PhysRevD.66.122002. URL: https://link.aps.org/doi/10.1103/PhysRevD.66.122002 (visited on 11/15/2023).

[2] Johan Samsing and Daniel J D'Orazio. "Black Hole Mergers From Globular Clusters Observable by LISA I: Eccentric Sources Originating From Relativistic N-body Dynamics". In: *Monthly Notices of the Royal Astronomical Society* 481.4 (Dec. 21, 2018), pp. 5445–5450. ISSN: 0035-8711, 1365-2966. DOI: 10.1093/mnras/sty2334. URL: https://academic.oup.com/mnras/article/481/4/5445/5087680 (visited on 11/17/2023).

[3] Michael Zevin et al. "Eccentric Black Hole Mergers in Dense Star Clusters: The Role of Binary–Binary Encounters". In: *The Astrophysical Journal* 871.1 (Jan. 24, 2019). Publisher: IOP Publishing, p. 91. ISSN: 0004-637X. DOI: 10.3847/1538-4357/aaf6ec. URL: https://iopscience.iop.org/article/10.3847/1538-4357/aaf6ec/meta (visited on 11/17/2023).

[4] Nicolas Yunes et al. "Post-circular expansion of eccentric binary inspirals: Fourier-domain waveforms in the stationary phase approximation". In: *Physical Review D* 80.8 (Oct. 1, 2009). Publisher: American Physical Society, p. 084001. DOI: 10.1103/PhysRevD.80.084001. URL: https://link.aps.org/doi/10.1103/PhysRevD.80.084001 (visited on 11/17/2023).

[5] J. W. Armstrong, F. B. Estabrook, and Massimo Tinto. "Time-Delay Interferometry for Space-based Gravitational Wave Searches". In: *The Astrophysical Journal* 527.2 (Dec. 20, 1999), pp. 814–826. ISSN: 0004-637X, 1538-4357. DOI: 10.1086/308110. URL: https://iopscience.iop.org/article/10.1086/308110 (visited on 11/15/2023).

[6] Lionel London et al. "First Higher-Multipole Model of Gravitational Waves from Spinning and Coalescing Black-Hole Binaries". In: *Phys. Rev. Lett.* 120 (16 Apr. 2018), p. 161102. DOI: 10.1103/PhysRevLett.120.161102. URL: https://link.aps.org/doi/10.1103/PhysRevLett.120.161102.

[7] Tousif Islam et al. "Eccentric binary black hole surrogate models for the gravitational waveform and remnant properties: comparable mass, nonspinning case". In: *Physical Review D* 103.6 (Mar. 16, 2021), p. 064022. ISSN: 2470-0010, 2470-0029. DOI: 10.1103/PhysRevD.103.064022. arXiv: 2101.11798[astro-ph,physics:gr-qc]. URL: http://arxiv.org/abs/2101.11798 (visited on 10/30/2023).

[8] Han Wang et al. *The Challenge of Eccentricity when Observing Stellar-mass Binary Black Holes with Space-Based Gravitational Wave Detectors*. Apr. 20, 2023. arXiv: 2304.10340[astro-ph,physics:gr-qc]. URL: http://arxiv.org/abs/2304.10340 (visited on 11/03/2023).

[9] Karl Martel and Eric Poisson. "Gravitational waves from eccentric compact binaries: Reduction in signal-to-noise ratio due to nonoptimal signal processing". In: *Physical Review D* 60.12 (Nov. 15, 1999), p. 124008. ISSN: 0556-2821, 1089-4918. DOI: 10.1103/PhysRevD.60.124008. arXiv: gr-qc/9907006. URL: http://arxiv.org/abs/gr-qc/9907006 (visited on 11/17/2023).

[10] Danilo Chiaramello and Alessandro Nagar. "Faithful analytical effective-one-body waveform model for spin-aligned, moderately eccentric, coalescing black hole binaries". In: *Phys. Rev. D* 101 (10 May 2020), p. 101501. DOI: 10.1103/PhysRevD.101.101501. URL: https://link.aps.org/doi/10.1103/PhysRevD.101.101501.

[11] Michael Katz. *lisa-on-gpu: Using GPU to compute LISA response to gravitational waves in millisecond scale*. en.

[12] P. C. Peters. "Gravitational Radiation and the Motion of Two Point Masses". In: *Physical Review* 136.4 (Nov. 23, 1964). Publisher: American Physical Society, B1224–B1232. DOI: 10.1103/PhysRev.136.B1224. URL: https://link.aps.org/doi/10.1103/PhysRev.136.B1224 (visited on 11/17/2023).

[13] Kallol Dey et al. "Effect of data gaps on the detectability and parameter estimation of massive black hole binaries with LISA". In: *Physical Review D* 104.4 (Aug. 2021). ISSN: 2470-0029. DOI: 10.1103/physrevd.104.044035. URL: http://dx.doi.org/10.1103/PhysRevD.104.044035.

[14] Olaf Hartwig and Martina Muratore. "Characterization of Time Delay Interferometry combinations for the LISA instrument noise". In: *Physical Review D* 105.6 (Mar. 25, 2022), p. 062006. ISSN: 2470-0010, 2470-0029. DOI: 10.1103/PhysRevD.105.062006. arXiv: 2111.00975[gr-qc]. URL: http://arxiv.org/abs/2111.00975 (visited on 11/15/2023).